Spectroscopic Characterization and O_2 Reactivity of the Trinuclear Cu Cluster of Mutants of the Multicopper Oxidase Fet3p†

Amy E. Palmer,‡ Liliana Quintanar,‡ Scott Severance,§ Tzu-Pin Wang,§ Daniel J. Kosman,*,§ and Edward I. Solomon*,‡

Department of Chemistry, Stanford University, Stanford, California 94305, and Department of Biochemistry, School of Medicine and Biomedical Sciences, State University of New York, Buffalo, New York 14214

Received October 29, 2001; Revised Manuscript Received April 1, 2002

ABSTRACT: Fet3p is a multicopper oxidase that uses four copper ions (one type 1, one type 2, and one type 3 binuclear site) to couple substrate oxidation to the reduction of O_2 to H_2O. The type 1 Cu site shuttles electrons between the substrate and the type 2/type 3 Cu sites which form a trinuclear Cu cluster that is the active site for O_2 reduction. This study extends the spectroscopic and reactivity studies that have been conducted with type 1-substituted Hg (T1Hg) laccase to Fet3p and a mutant of Fet3p in which the trinuclear Cu cluster is perturbed. To examine the reaction between the trinuclear Cu cluster and O_2, the type 1 Cu Cys_{484} was mutated to Ser, resulting in a type 1-depleted (T1D) form of the enzyme. Additional His to Gln mutations were made at the trinuclear cluster to further probe specific contributions to reactivity. One of these mutants ($His_{126}Gln$) produces the first stable but perturbed trinuclear Cu cluster (T1DT3′ Fet3p). Spectroscopic characterization (absorption, circular dichroism, magnetic circular dichroism, and electron paramagnetic resonance) of the resting trinuclear sites in T1D and T1DT3′ Fet3p reveal that the $His_{126}Gln$ mutation changes the electronic structure of both the type 3 and type 2 Cu sites. The trinuclear clusters in T1D and T1DT3′ Fet3p react with O_2 to produce peroxide intermediates analogous to that observed in T1Hg laccase. Spectroscopic data on the peroxide intermediates in the three forms provide further insight into the structure of this intermediate. In T1D Fet3p, the decay of this peroxide intermediate is pH-dependent, and the rate of decay is 10-fold higher at low pH. In T1DT3′ Fet3p, the decay of the peroxide intermediate is pH-independent and is slow at all pH's. This change in the pH dependence provides new insight into the mechanism of intermediate decay involving reductive cleavage of the O−O bond.

Multicopper oxidases are an important class of enzymes in bacteria, fungi, plants, and animals. Well-known members of this class include laccase, ascorbate oxidase (AO),[1] ceruloplasmin (Cp), and Fet3p (*1*). Fet3p is a plasma membrane protein that was originally isolated from *Saccharomyces cerevisiae* (*2, 3*). In vivo Fet3p is associated with the iron permease, Ftr1p. Together, Fet3p and Ftr1p have been shown to play an integral role in high-affinity iron uptake in yeast; Fet3p appears to oxidize Fe^{2+} to Fe^{3+} while Ftr1p is required for the transport of Fe^{3+} across the plasma membrane (*4, 5*).

All multicopper oxidases utilize at least four Cu ions to couple the four-electron reduction of O_2 to H_2O with four sequential one-electron substrate oxidations. The four Cu ions are classified into three types of sites based on the spectroscopic properties they exhibit in the oxidized (Cu^{2+}) state. The type 1 (T1) Cu site is characterized by an intense (∼5000 M^{-1} cm^{-1}) Cys → Cu charge-transfer transition at ∼600 nm and small ($<100 \times 10^{-4}$ cm^{-1}) parallel hyperfine coupling in electron paramagnetic resonance (EPR). The T1 Cu tends to dominate the absorption (abs), circular dichroism (CD), and magnetic circular dichroism (MCD) spectrum of multicopper oxidases. The primary function of this site is long-range electron transfer, and in multicopper oxidases, it is responsible for shuttling electrons from substrate to the remaining Cu sites (∼13 Å away) (*1*).

The type 2 (T2) Cu site does not have any distinctive abs features but can be studied by EPR (parallel hyperfine coupling $\sim 200 \times 10^{-4}$ cm^{-1}) and MCD at low temperature. The type 3 (T3) Cu site is comprised of two Cu ions that are antiferromagnetically coupled through a bridging hydroxide. The resulting diamagnetic ($S_{total} = 0$) site does not have an EPR signal but exhibits a charge-transfer transition ∼330 nm in abs as well as a series of ligand field transitions in the CD spectrum. Together the T2 and T3 Cu sites form a trinuclear Cu cluster which is the site of O_2 binding and reduction (*1, 6*).

Most studies on the catalytic cycle of multicopper oxidases have focused on laccase because of its simplicity. Under both

† This research was supported by NIH Grant DK31450 to E.I.S. and NIH Grant DK53820 to D.J.K. A.E.P. was a Franklin Veatch Memorial Fellow at Stanford University.

* To whom correspondence should be addressed. E.I.S.: phone: (650) 723-9104, e-mail: edward.solomon@stanford.edu. D.J.K.: phone: (716) 829-2842, e-mail: camkos@acsu.buffalo.edu.

‡ Stanford University.

§ State University of New York.

[1] Abbreviations: T1, type 1; T2, type 2; T3, type 3; T1D, type 1 depleted; T1DT3′, type 1-depleted/H126Q mutant; T1Hg laccase, type 1-substituted Hg laccase; AO, ascorbate oxidase; Cp, ceruloplasmin; EPR, electron paramagnetic resonance; abs, absorption; CD, circular dichroism; MCD, magnetic circular dichroism; CT, charge transfer; **P**, peroxide intermediate.

10.1021/bi011979j CCC: $22.00
Published on Web 04/27/2002

single-turnover and steady-state conditions, fully (four-electron) reduced *Rhus vernicifera* laccase has been shown to react with O_2 to produce a transient species that decays to the resting, oxidized enzyme ($k = 0.03$ s^{-1}, 25 °C, pH 7.4) (*7*−*9*). This transient species is referred to as the native intermediate, **N**. Extensive spectroscopic studies on **N** reveal that all four electrons (one from each Cu) are transferred to dioxygen, resulting in a fully oxidized enzyme in which the trinuclear Cu site is bridged by the fully reduced oxygen product (*10*). The structure of **N** differs from that of the resting, oxidized enzyme because the latter does not have an all-bridged trinuclear cluster.

Additional insight into the mechanism of O_2 reduction has been obtained from studies on a derivative of laccase in which the T1 Cu was removed and replaced by a spectroscopically silent and redox-inactive Hg^{2+} ion (*11*−*13*). This T1Hg laccase retains a competent trinuclear cluster that reacts with O_2. The reaction of fully (three-electron) reduced T1Hg laccase with O_2 has been shown to produce a peroxide intermediate (**P**) in which the peroxide bridges between the reduced T2 Cu and the oxidized T3 Cu sites (*14*). A combination of spectroscopic and kinetic isotope studies revealed that **P** decays via electron transfer from the T2 Cu and cleavage of the peroxide O−O bond (*14*, *15*). Reductive cleavage of the O−O bond in **P** leads to the formation of an **N**-like species that decays to resting, oxidized T1Hg laccase, suggesting that this peroxide intermediate lies on the catalytic reaction coordinate. Subsequent studies on this peroxide intermediate seem to support this initial observation (*16*, *17*). The studies on T1Hg and native laccase suggest that the four-electron reduction of O_2 to H_2O proceeds via 2 two-electron steps; the first step results in formation of a peroxide level species while the second produces the fully reduced product.

The present study extends these mechanistic investigations to T1-depleted (T1D) Fet3p. In T1D Fet3p, one of the T1 Cu ligands, Cys_{484}, is mutated to Ser, thus preventing incorporation of Cu into this site (*3*, *18*). The T2 and T3 Cu sites are unaffected by the $Cys_{484}Ser$ mutation, and therefore T1D Fet3p retains a competent trinuclear cluster. Because Fet3p has been cloned, expressed, and isolated, this system affords the opportunity for perturbation of the Cu sites and surrounding residues through site-directed mutagenesis. A number of mutants have been prepared in which the trinuclear Cu His ligands are changed to Gln. One of these mutants generates the first stable but perturbed trinuclear cluster, while in the remaining mutants the trinuclear cluster fails to form (*19*). This study investigates the impact that this novel mutant [T1DT3′, in which one of the T3 Cu ligands (H_{126}) has been changed to Gln] has on the electronic structure of the resting trinuclear Cu cluster in T1D Fet3p and its reaction with O_2. The reaction of T1D and T1DT3′ Fet3p with O_2 is examined and compared to T1Hg laccase. Comparison of the nature and behavior of the oxygen intermediates in T1D and T1DT3′ Fet3p provides new insight into interactions which influence the O_2 reactivity of the trinuclear Cu cluster.

EXPERIMENTAL PROCEDURES

Expression, isolation, purification, and characterization of soluble T1D Fet3p were performed as described previously (*3*, *18*). A series of trinuclear mutants were prepared in an attempt to perturb the T2 and T3 Cu centers but maintain an intact trinuclear cluster. The first mutant, $H_{128}Q$, yielded protein with only 2.1 Cu/protein, no absorbance at 330 nm and reduced absorbance at 608 nm. The second mutant, $H_{81}Q$, yielded 3 Cu/protein, and EPR and MCD indicated that the T2 Cu was not present (*19*). The third trinuclear mutant, $H_{126}Q$, yielded 3.8 Cu/protein with normal absorption at 330 nm, indicating that the protein contained a stable and intact trinuclear cluster. Therefore, a double mutant of Fet3p containing the $C_{484}S$ mutation and $H_{126}Q$ mutation was prepared. The present study focuses on this $C_{484}S/H_{126}Q$ mutant, referred to as T1DT3′. The mutant gene was constructed directly in the plasmid encoding the T1D mutant [the $C_{484}S$ mutant, ref (*18*)] using the QuickChange mutagenesis kit from Stratagene and the appropriate pair of mutagenic primers. This plasmid was derived from pDY148 that contained a truncated form of the *FET3* gene to which sequences encoding the FLAG epitope were appended (*3*). This vector, and all those derived from it, produced a Fet3 protein in yeast that lacked its C-terminal, membrane anchor and was secreted directly into the culture medium (*3*). Fet3 proteins produced in this way were readily purified to homogeneity from the medium by three passes over a MonoQ column with salt elution (*3*, *18*). Typically, this procedure yielded 3−6 mg of pure Fet3p per liter of growth medium (*3*). The Cu content of T1D and T1DT3′ was measured spectrophotometrically using 2,2′-biquinoline (*20*) or by atomic absorption spectroscopy and typically ranged from 2.9 to 3.3 Cu/protein.[2] The protein concentration of each preparation was determined using the Bradford assay. By comparison of the absorption spectrum and protein concentration of different T1D and T1DT3′ samples, the ϵ_{330nm} was determined to be 4.57 and 4.21 mM^{-1} cm^{-1}, respectively.[3] Once it was determined that the ϵ_{330} was comparable in both enzymes, this band was used to determine the protein concentration of a sample for a given experiment. The concentration of paramagnetic Cu was determined from spin quantitation of EPR spectra. Both T1D and T1DT3′ typically contained 30−35% paramagnetism, as expected. All chemicals were reagent grade and were used without further purification. Water was purified to a resistivity of 15−18 MΩ cm^{-1} using a Barnstead Nanopure deionizing system.

All spectroscopic characterization was performed in 100 mM potassium phosphate buffer, pH 7.5. For CD and MCD experiments, samples were prepared in deuterated buffer (100 mM potassium phosphate in 99.99% D_2O, pD 7.5). Glassed samples for MCD experiments were prepared by adding 50% (v/v) buffer/glycerol-d_3. Addition of glycerol had no effect on the CD spectrum of the enzymes.

Room temperature UV−visible absorption spectra were recorded using a Hewlett-Packard HP8452A diode array spectrophotometer. Room temperature CD and low-temperature (5 K) MCD spectra in the UV−visible region were collected with a Jasco J-810-150S spectropolarimeter operating with an S-20 photomultiplier tube and an Oxford SM4-7T magnet. CD and MCD spectra in the near-IR region were obtained with a Jasco J-200-D spectropolarimeter, a liquid nitrogen cooled InSb detector, and an Oxford SM4000-7T

[2] The wild-type protein typically contained 3.7−3.9 Cu/protein.

[3] The ϵ_{280} for T1D was 135 mM^{-1} cm^{-1} and for T1DT3′ was 122 mM^{-1} cm^{-1}. The 280/330 ratio was 29.5 in T1D and 29 in T1DT3′.

magnet. CD samples were run in a 1.0 cm quartz cuvette. MCD samples were run in cells fitted with quartz disks and a 3 mm rubber spacer. Gaussian fitting of the abs, CD, and MCD spectra was performed using PeakFit 4.0 (Jandel). Gaussian analyses of the absorption and CD spectra were performed as followed: the same parameters (energy and bandwidth) were used to fit both the absorption and CD in order to help constrain the fit. The minimum number of bands was used to adequately fit key features in both spectra. EPR spectra were obtained using a Bruker EMX spectrometer, ER 041 XG microwave bridge, and ER 4102ST cavity. All X band samples were run at 77 K in a liquid nitrogen finger dewar. A Cu standard (1.0 mM $CuSO_4 \cdot 5H_2O$ with 2 mM HCl and 2 M $NaClO_4$) (*21*) was used for spin quantitation of the EPR spectra. Q band spectra were obtained at 77 K using an ER 051 QR microwave bridge, an ER 5106QT resonator, and an Oxford continuous flow CF935 cryostat. EPR spectra were baseline-corrected and simulated using XSophe (Bruker). For a given enzyme, X and Q band spectra were simultaneously fit in order to constrain the simulation parameters (using the same *g* values and hyperfine constants allowed more accurate assessment of the line widths). In the fits presented, the line widths were optimized using a model that accounts for *g* and *A* strain.

Peroxide intermediate experiments were performed at room temperature (25 °C) in either 100 mM MES or 100 mM potassium phosphate buffer. For pH 4.7, 5.0, 5.5, and 6.5, MES was used while at pH 7.5 phosphate buffer was used. The protein was exchanged into buffer of the desired pH using Amicon concentrators. Previous studies have shown that the rate of decay of the intermediate at a given pH is the same in MES and phosphate buffer (*15*). The intermediate was prepared as described previously (*15*) in a Vacuum Atmospheres Nexus-1 anerobic glovebox with the following changes. The dithionite was exchanged out of the reduced protein solution by extensive washing (microcon-30, Amicon) with degassed buffer of the appropriate pH in the glovebox. The reduced protein (250 μL of either T1D or T1DT3′) was placed in a 1 cm path length cuvette fitted with a septum and was cycled out of the glovebox. O_2-saturated buffer (250 μL of the appropriate pH) was then added, and the spectrum was recorded on an HP8452A spectrophotometer. The final protein concentrations were typically 0.045−0.05 mM, and the final O_2 concentration was estimated to be 0.5 mM (*22*).

RESULTS AND ANALYSIS

Mutations at the Trinuclear Cluster. To better understand the nature of the trinuclear Cu cluster and its reaction with O_2, we prepared mutants of Fet3p in which a number of histidines (H_{126}, H_{128}, and H_{81}) were changed to glutamine (Q). Figure 1 shows the trinuclear cluster of *Cucurbita pepo medullosa* ascorbate oxidase (AO), and Table 1 lists selected portions of the amino acid sequences of AO, *Coprinus cinereus* laccase (CcL), *Trametes versicolor* laccase,[4] and Fet3p. As can be seen from the crystal structure and sequence comparison, H_{126}, H_{128}, and H_{81} correspond to histidine residues that are ligands of the T3 Cu_α, T3 Cu_β, and T2 Cu, respectively.

[4] *Trametes versicolor* laccase is a characteristic fungal laccase. It should be noted that this enzyme has been called *Polyporus versicolor* and *Coriolus versicolor* in the past.

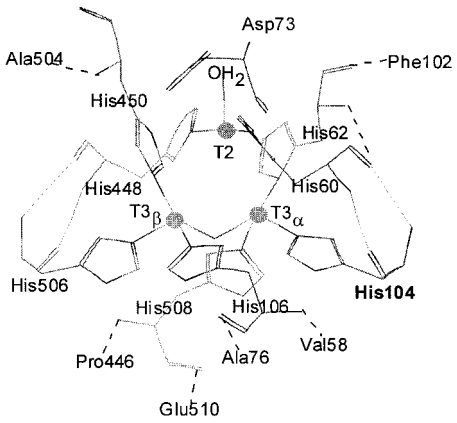

FIGURE 1: Trinuclear cluster in ascorbate oxidase, taken from the X-ray crystal structure (*35*). The T2 and the T3 Cu ions are shown along with their coordinating residues. Hydrogen bonds in the vicinity of the trinuclear cluster are depicted by the dashed lines. The His which corresponds to the mutated His in T1DT3′ Fet3p is indicated in boldface type. It is one of the ligands of T3 Cu_α and is H-bonded to one of the T2 Cu ligands. The distance between the T2 Cu−OH(H) and Asp73 would depend on the pH of the crystal.

Table 1: Sequence Comparison[a]

			T2		T3				T3		T3
AO	V_{58}	I_{59}	H_{60}	W_{61}	H_{62}	D_{73}	A_{76}	F_{102}	H_{104}	G_{105}	H_{106}
CcL	S_{62}	I_{63}	H_{64}	W_{65}	H_{66}	D_{77}	D_{80}	W_{107}	H_{109}	S_{110}	H_{111}
TvL	S_{83}	I_{84}	H_{87}	W_{88}	H_{89}	D_{98}	A_{101}	W_{128}	H_{132}	S_{133}	H_{134}
Fet3	S_{79}	M_{80}	H_{81}	F_{82}	H_{83}	D_{94}	P_{97}	W_{124}	H_{126}	S_{127}	H_{128}

	T2			T3	T3	(T1)	T3		
AO	P_{446}	H_{448}	L_{449}	H_{450}	H_{506}	C_{507}	H_{508}	I_{509}	E_{510}
CcL	P_{397}	H_{399}	L_{400}	H_{401}	H_{451}	C_{452}	H_{453}	I_{454}	E_{455}
TvL	P_{417}	H_{427}	L_{428}	H_{429}	H_{479}	C_{480}	H_{481}	I_{482}	D_{483}
Fet3	P_{414}	H_{416}	L_{417}	H_{418}	H_{483}	C_{484}	H_{485}	I_{486}	E_{487}

[a] Abbreviations: AO, *Cucurbita pepo medullosa* ascorbate oxidase [ref (*36*), accession no. 442635]; CcL, *Coprinus cinereus* laccase [ref (*37*), accession no. 1A65]; TvL, *Trametes versicolor* laccase [ref (*38*), accession no. 2598857]; Fet3, *Saccharomyces cerevisiae* Fet3 [ref (*4*), accession no. L25090].

The $H_{81}Q$ mutant in Fet3p resulted in a T2-depleted form of the enzyme, as characterized previously (*18*, *19*). The $H_{128}Q$ mutant only contained 2.1 Cu/protein and showed no absorbance at 330 nm, indicating that this mutation also adversely affected incorporation of Cu into the trinuclear cluster. Because these mutants do not contain an intact trinuclear cluster, further spectroscopic characterization was not pursued. In contrast to these cluster mutants, the $H_{126}Q$ mutant yielded protein with a stable trinuclear cluster (with 3.8 Cu/protein and normal absorption at 330 nm). Therefore, the $C_{484}S/H_{126}Q$ double mutant of Fet3p was prepared, yielding protein with three Cu ions, the same as T1D Fet3p. From Table 1, H_{126} corresponds to H_{104} in AO, and is one of the T3 Cu_α-ligating histidines (Figure 1). In addition, H_{126} is likely hydrogen-bonded to H_{81} (H_{60} in AO, one of the T2 Cu-ligating histidines).[5] To gain insight into how this mutation influences the electronic structure of the trinuclear Cu site, spectroscopic studies were carried out on T1D and T1DT3′ Fet3p at pH 7.5.[6]

Nature of the T3 Cu Site in T1D and T1DT3′ Fet3p. The absorption and CD spectra of multicopper oxidases are dominated by T1 and T3 Cu transitions (*23*, *24*). Upon

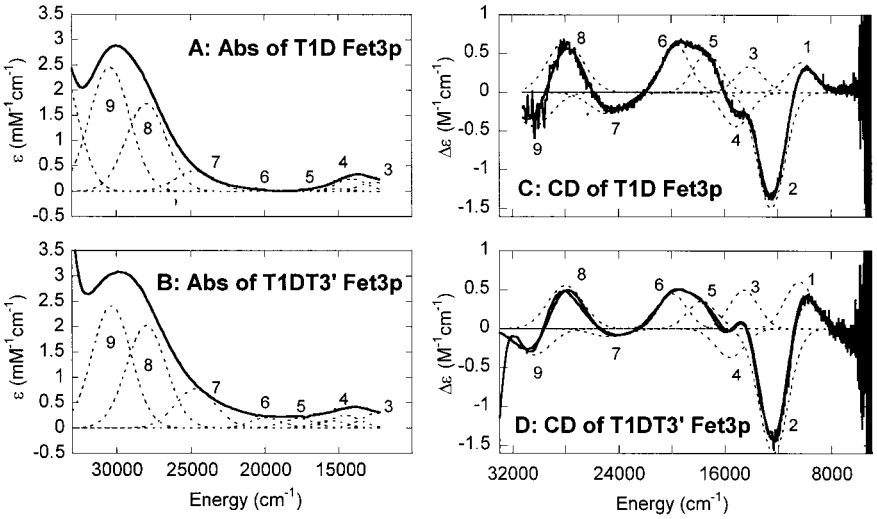

FIGURE 2: Room temperature absorption spectra of T1D (A) and T1DT3′ (B) Fet3p. CD spectra of T1D (C) and T1DT3′ (D) Fet3p. Also indicated are the individual Gaussian bands.

removal of the T1 Cu, the T3 Cu is the primary contributor to the absorption and CD spectra. Figure 2A,B presents the absorption spectrum of T1D and T1DT3′ Fet3p, respectively. There is an intense ($\epsilon \sim 4.2$ mM^{-1} cm^{-1}) transition at ~30 300 cm^{-1}. Previous studies on laccase and wild-type Fet3p have assigned this transition as a μ-OH → Cu^{2+} charge transfer (CT) (*1*, *19*). The energy and intensity of this transition are comparable in T1D and T1DT3′, indicating that the interaction of the OH bridge and the T3 Cu atoms is intact upon mutation of H_{126} to Q. The weak absorption bands at ~740 nm (~13 500 cm^{-1}) are ligand field transitions of the T3 Cu.

The CD spectra of T1D and T1DT3′ Fet3p are shown in Figure 2C,D, respectively. Overall, the energy and intensity of the bands are quite similar in T1D and T1DT3′. A decrease in coordination number would be expected to significantly perturb the ligand field as well as shift the charge-transfer transitions down in energy. The fact that the two spectra are so similar indicates that the coordination number of both T3 Cu ions (Cu_α and Cu_β) is similar in T1D and T1DT3′ Fet3p. Consequently, in T1DT3′ the glutamine (Q_{126}) likely coordinates to the T3 Cu_α. The CD spectrum of T1DT3′ does not change as a function of pH (from 5.5 to 7.5), suggesting that the carbonyl oxygen of the Gln replaces the His as one of the T3 Cu_α ligands.

Gaussian analysis of the absorption and CD spectra was performed as described under Experimental Procedures. This simultaneous Gaussian fitting requires the presence of nine bands in the energy region from 5000 to 33 000 cm^{-1}. The individual Gaussian bands are included in Figure 2 and presented in Table 2. The six transitions below 20 000 cm^{-1} (bands 1−6) have been assigned as T3 Cu ligand field bands in T1Hg-substituted laccase (*25*), and the similarity between the CD spectrum of T1Hg laccase and the T1D Fet3p proteins suggests this assignment is appropriate in Fet3p as well. Additionally, the Kuhn anisotropy factor, i.e., the ratio of CD to absorption intensity ($\Delta\epsilon/\epsilon$, Table 2), is much higher for bands 1−6, consistent with their assignment as ligand field transitions (*26*, *27*). The fact that more than four ligand field transitions exist indicates that the two T3 Cu ions are inequivalent.

The energy and low Kuhn anisotropy factors of the three transitions at energies higher than 20 000 cm^{-1} suggest they

Table 2: Comparison of Gaussian Fits

band no.	T1D, energy/ϵ[a]	T1D, $\Delta\epsilon/\epsilon$[b]	T1DT3′, energy/ϵ[a]	T1DT3′, $\Delta\epsilon/\epsilon$[b]
	Abs/CD: T3 Cu			
1	10200/ND	ND	10400/ND	ND
2	12500/0.177	−8.41	12350/0.304	−5.25
3	14080/0.242	1.39	14550/0.251	1.98
4	15120/0.046	−9.47	15600/0.142	−2.56
5	17300/0.027	18.9	17720/0.187	1.91
6	19630/0.019	31.2	19930/0.201	2.24
7	24770/0.400	−0.68	24700/0.775	−0.13
8	28000/1.73	0.38	28000/2.01	0.28
9	30400/2.45	−0.18	30350/2.41	−0.14
	MCD: T2 Cu			
band no.	energy/nm		energy/nm	
1 *xy*	9700/1031		9700/1031	
2 *xz*	12000/833		11700/855	
3 *yz*	13900/719		14000/714	
4 z^2	16800/595		17000/588	
5 His π	20150/496		19800/505	
6 His π	24900/402		24800/403	
7 His π	28200/355		28700/348	
8 His π	30750/325		31000/323	

[a] The energy of the transitions is reported in cm^{-1}, and the extinction coefficient of the absorption bands is reported in mM^{-1} cm^{-1}. The energy was obtained from simultaneously fitting the CD and the difference absorption spectrum. The difference absorption spectrum (oxidized − reduced spectrum) was used in order to subtract off the protein absorption band at 280 nm. [b] Kuhn anisotropy factor calculated from the CD intensity ($\Delta\epsilon$) in M^{-1} cm^{-1} and the absorption intensity (ϵ) in M^{-1} cm^{-1}. Expressed as $X \times 10^{-3}$.

[5] Comparable hydrogen bonds are observed in *Coprinus cinereus* laccase (*37*) and ceruloplasmin (*39*).

[6] We have pursued extensive pH studies on T1D Fet3p and T1Hg laccase to evaluate whether there are any changes in the spectral features of the T2 Cu upon converting its bound H_2O to OH (*28*). Analogous pH studies could not be conducted with T1DT3′ because at low pH, a small amount of a second paramagnetic species forms. This second species does not exhibit properties of the T2 Cu in the trinuclear cluster (it does not bind F^- and does not react with O_2 to produce a peroxide intermediate) and appears to be a non-native form of the enzyme that likely results from a conformational change. This second species contributes to the EPR and MCD spectra of T1DT3′ at low pH and therefore complicates spectral comparison.

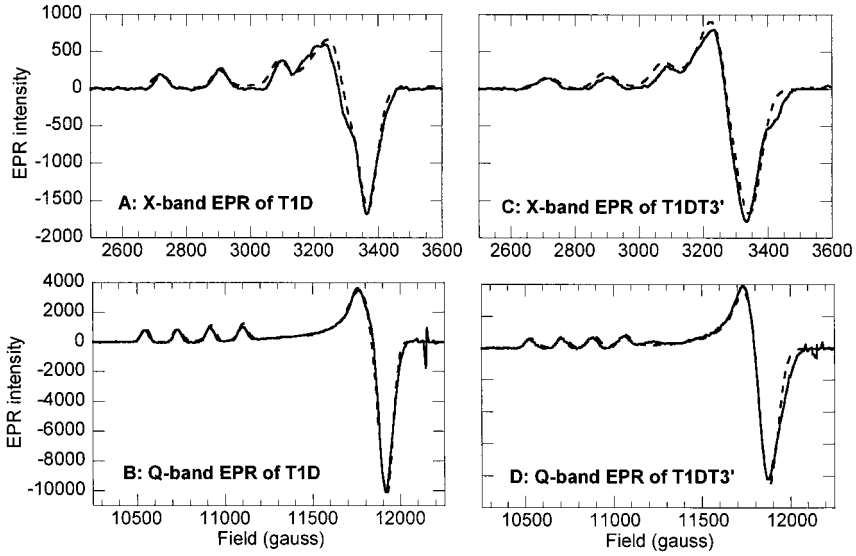

FIGURE 3: EPR spectra of T1D and T1DT3′ Fet3p at 77 K. (A) X band and (B) Q band EPR spectra of T1D. (C) X band and (D) Q band EPR spectra of T1DT3′. Experimental spectra (solid lines) and simulated spectra obtained with the parameters listed in Table 3 (dotted lines) are shown. All spectra were collected at 77 K. The X band spectra were recorded under the following conditions: 9.4040 or 9.4126 GHz microwave frequency, 10.1 mW microwave power, 100 kHz modulation frequency, 20 G modulation amplitude, 81.92 ms conversion time, 327 ms time constant. 5 scans were averaged to obtain the spectra presented in (A) and (C). The Q band spectra were recorded under the following conditions: 34.00 GHz microwave frequency, 13 dB attenuation, 100 kHz modulation frequency, 10 G modulation amplitude, 163 ms conversion time, 327 ms time constant. 6 scans were averaged to obtain the spectra presented in (B) and (D).

are ligand to metal charge-transfer (CT) transitions. The CD data show that the 330 nm absorption band is actually composed of two bands (bands 8 and 9), consistent with μ-OH CT transitions to the two T3 coppers (*28*). Band 7 can be reasonably assigned as a His $\pi \rightarrow$ Cu CT transition. This His $\rightarrow$ Cu CT is much lower in energy ($\sim$5000 cm^{-1}) than observed for 4-coordinate tetragonal Cu complexes (*29*, *30*) but is at the same energy as one of the His $\rightarrow$ T2 Cu CT transitions in MCD (vide infra) (*28*). Therefore, this transition can be assigned as a His $\rightarrow$ T2 Cu CT. There is no difference in the CT region of T1D and T1DT3′.

The main difference in the CD spectrum of T1D and T1DT3′ occurs in the ligand field region. The transition energies of bands 3, 4, and 5 increase significantly (+500, 400, and 300 cm^{-1}, respectively) in T1DT3′. An increase in transition energy results from stabilization of the relevant d orbital relative to the half-filled HOMO. The carbonyl oxygen of Gln is expected to be a weaker donor ligand than the imidazole nitrogen it replaces in the mutant. From the CD spectrum, it is clear that one of the d $\rightarrow$ d transitions of T1DT3′ (band 3) is more strongly perturbed than the others. Ligand field calculations show that the T3 Cu has a half-filled d_{z^2} ground state and approximate trigonal bipyramidal geometry (with an open coordination position in the equatorial plane) (*25*). In Fet3p, His_{83} and His_{126} make up the equatorial (*xy*) plane. Therefore, the d_{xy} and $d_{x^2-y^2}$ orbitals would be most affected by changes in ligand coordination in the *xy* plane, and d_{xy} has the most overlap with the histidine ligands.[7] Hence, band 3 represents the $d_{xy} \rightarrow d_{z^2}$ transition of T3 Cu_α.

Nature of the T2 Cu Site in T1D and T1DT3′ Fet3p. Because the T3 Cu site is diamagnetic, only the T2 Cu will contribute to the EPR spectrum of T1D Fet3p. EPR spectra were collected at X band ($\sim$9.5 GHz) and Q band ($\sim$34 GHz) to resolve the *g* values and hyperfine coupling constants, *A* (Figure 3). The X and Q band spectra were simultaneously simulated in order to obtain the ground-state spin Hamiltonian parameters for T1D and T1DT3′ Fet3p (Table 3). The EPR spectra of T1D and T1DT3′ are quite similar, but there are small changes in the *g* values and hyperfine coupling constants, indicating that in T1DT3′ Fet3p the T2 Cu is perturbed by the $H_{126}Q$ mutation at the T3 Cu site.

Table 3: Comparison of EPR Parameters

	T1D	T1DT3′
g_x	2.041	2.052
A_x	15−20[a]	≤10
g_y	2.055	2.063
A_y	10−20[a]	≤10
g_z	2.243	2.253
A_z	190 ± 2	183 ± 2

[a] For the EPR simulations shown in Figure 3, $A_x = 17$ and $A_y = 15$. The line widths used were as follows: for T1D, $L_x = 30/32$, $L_y = 43/59$, and $L_z = 28/28$, for X band and Q band, respectively; and for T1DT3′: $L_x = 40/55$, $L_y = 45/67$, and $L_z = 38/38$, for X band and Q band, respectively. The hyperfine coupling constants and line widths are reported in $X \times 10^{-4}$ cm^{-1}.

The *g* values of the T2 site in T1DT3′ Fet3p are higher than those in T1D Fet3p. From the *g* value expressions obtained from ligand field theory (*31*), the *g* values are directly proportional to the amount of metal character in the half-occupied HOMO (i.e., covalency) and inversely proportional to the ligand field transition energies. For the *g* values of T1DT3′ to be higher than T1D, there must be a decrease in in the ligand field or an increase in covalency. From the MCD spectra (vide infra), the ligand field of T1DT3′ is slightly higher than T1D, and the increase in *g* values cannot be explained by a change in ligand field. Therefore, there must be a decrease in the T2 site covalency in T1DT3′ as compared to T1D.

[7] The coordinate system is defined such that the Cu and the T3-His N ligands form the *x*,*y*-plane and the *y* axis is oriented along the open coordination position.

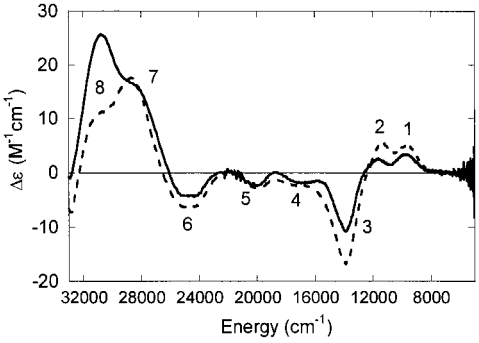

FIGURE 4: Low-temperature (5 K) MCD spectrum of T1D (solid line) and T1DT3′ (dashed line). The 0T baseline was subtracted from the 7T scan to obtain the spectra presented above.

From the parameters listed in Table 3, it is evident that for the T2 Cu the magnitude of A_z has decreased with the $H_{126}Q$ mutation. There are three contributions to the hyperfine coupling constant which are given by the general expression (*31*):

$$A = A^{\text{Fermi}} + A^{\text{Spin Dipolar}} + A^{\text{Orbital Dipolar}}$$

The higher g values in T1DT3′ increase the orbital dipolar contribution to the hyperfine (which is positive) and decrease the magnitude of the hyperfine coupling (which is negative). The decreased covalency of T1DT3′ would impact the Fermi contact and spin dipolar contributions to the hyperfine and would be expected to increase the magnitude of the hyperfine coupling constant. If the experimental g values of T1DT3′ are used to estimate the hyperfine coupling constants, assuming that all other contributions are the same as in T1D, the following hyperfine coupling constants are obtained: $A_x \simeq -13 \times 10^{-4}$ cm^{-1}, $A_y \simeq -13 \times 10^{-4}$ cm^{-1}, and $A_z \simeq -184 \times 10^{-4}$ cm^{-1}. The experimental values are $A_x \leq |10| \times 10^{-4}$ cm^{-1}, $A_y \leq |10| \times 10^{-4}$ cm^{-1}, and $A_z = |183| \times 10^{-4}$ cm^{-1}. Therefore, it is evident that the increased experimental g values account for the decrease in A_z observed in the experimental EPR spectrum of T1DT3′.

Low-temperature MCD follows C-term selection rules and specifically probes the paramagnetic T2 Cu site. Figure 4 shows the MCD spectrum of T1D and T1DT3′ Fet3p, and Table 2 presents the individual band energies of the MCD Gaussian fits. Overall these spectra are quite similar. The four lowest energy bands (1−4) are the ligand field transitions and have been assigned as d_{xy}, d_{xz}, d_{yz}, and d_{z^2} (in order of increasing energy) (*25*). As can be seen from Figure 4, the ligand field of T1D and T1DT3′ Fet3p is almost identical, with a slight increase in the energy of the d_{z^2} transition (band 4) and a decrease in the d_{xz} transition (band 2) in T1DT3′. There is also an increase in intensity of the ligand field transitions in T1DT3′. MCD C-term intensity derives from spin−orbit coupling of two orthogonally polarized transitions (*32*). The increase in intensity of the ligand field transitions of T1DT3′ results from increased mixing, consistent with the greater d character from the g values. The similar ligand field in T1D and T1DT3′ Fet3p suggests that the overall geometry of the T2 Cu site does not change significantly with the $H_{126}Q$ mutation.

The next four bands (5−8) in the MCD spectrum are ligand to metal charge-transfer transitions and have been assigned as His $\pi \rightarrow$ Cu $d_{x^2-y^2}$ transitions (*28*). There are

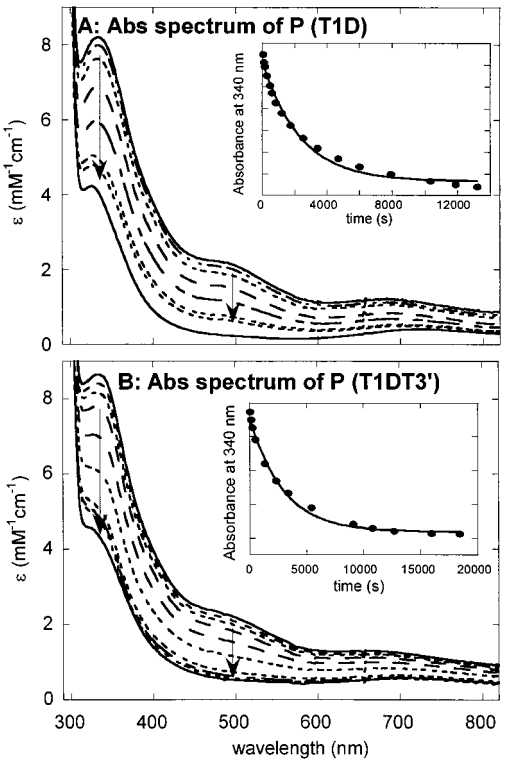

FIGURE 5: Absorption spectrum of the peroxide intermediate in (A) T1D Fet3p and (B) T1DT3′ Fet3p. The spectrum was recorded at room temperature in a 1 cm path length cuvette. For T1D, the peroxide intermediate was prepared in 100 mM MES, pH 6.5, buffer. For T1DT3′, the intermediate was prepared in 100 mM MES, pH 5.8, buffer. The absorption spectrum of **P** did not change with pH. The inset shows the absorbance at 340 nm as a function of time. Data were fit according to a single exponential.

two transitions (π_1 and π_2) from each His ligand. The largest difference in the charge-transfer region is the intensity decrease of the highest energy charge-transfer band (band 8) and the increase in intensity of band 6. As mentioned previously, in Fet3p H_{126} is likely to be hydrogen-bonded to the T2 Cu ligand H_{81}. If this hydrogen-bonding network is perturbed by the $H_{126}Q$ mutation, the bonding interaction between H_{81} and the T2 Cu could be altered, resulting in the intensity redistribution. The MCD data correlate well with the EPR data, and together these suggest the electronic structure of the T2 Cu has been altered in T1DT3′ Fet3p.

Nature of the Peroxide Intermediate in T1D and T1DT3′ Fet3p. It has previously been shown that reaction of reduced T1Hg laccase with O_2 produces a peroxide intermediate (**P**) that bridges between the reduced T2 Cu and the oxidized T3 Cu site (*14*). The current study extends this work to Fet3p. Reaction of 3e$^-$-reduced T1D Fet3p with O_2-saturated buffer (10-fold excess of O_2 over protein) results in the formation of a transient species with the absorption spectrum shown in Figure 5A. This transient species decays very slowly to resting, fully oxidized T1D Fet3p. The cycle can be repeated if more reducing equivalents are added. As with T1Hg laccase, formation of this intermediate in T1D was fast and complete at the time the first spectrum was collected (1 min). The absorption spectrum of this intermediate is analogous to that of T1Hg laccase, indicating a similar peroxide species is formed.

Parallel experiments were performed with T1DT3′ Fet3p to determine whether the perturbed trinuclear cluster would

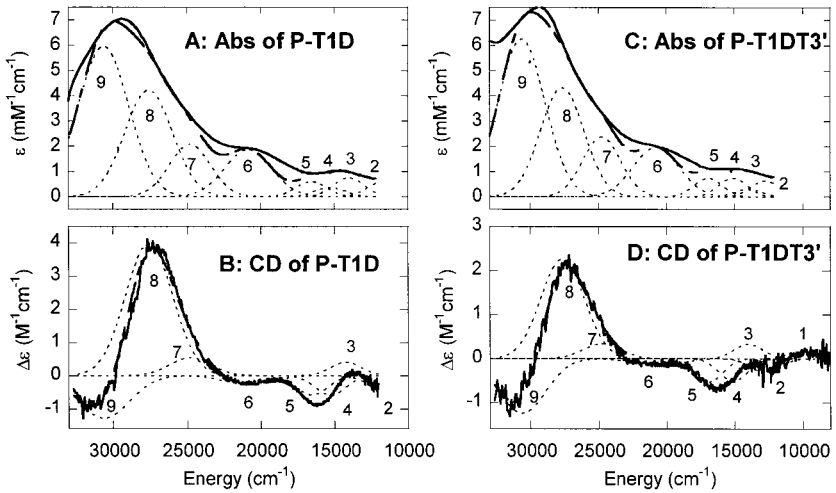

FIGURE 6: Room temperature difference absorption spectrum (A) and CD spectrum of the peroxide intermediate of T1D Fet3p (solid line) along with the individual Gaussian bands. Room temperature difference absorption spectrum (C) and CD spectrum (D) of the peroxide intermediate of T1DT3′ Fet3p (solid line) along with individual Gaussian bands. The difference absorption was obtained by subtracting the spectrum of the reduced protein from that of the peroxide intermediate. The intermediate CD spectra were recorded 90 s after reacting reduced enzyme with O_2.

Table 4: Comparison of Gaussian Fits for CD Spectrum **P** in T1D and T1DT3′

band no.	T1D, energy (cm^{-1})/ϵ ($mM^{-1}\,cm^{-1}$)	T1D, $\Delta\epsilon/\epsilon$[a]	T1DT3′, energy (cm^{-1})/ϵ ($mM^{-1}\,cm^{-1}$)	T1DT3′, $\Delta\epsilon/\epsilon$[a]
1	*b*	ND	(+) 10100/ND	ND
2	(−) 11690/0.59	−0.72	(−) 12760/0.64	−0.51
3	(+) 14230/0.76	0.54	(+) 14000/0.29	1.15
4	(−) 15280/0.36	−1.61	(−) 15120/0.75	−0.68
5	(−) 16540/0.59	−0.98	(−) 16920/0.75	−0.71
6	(−) 20850/1.86	−0.15	(−) 20750/1.97	−0.09
7	(+) 24800/2.07	0.26	(+) 24750/2.37	0.14
8	(+) 27580/4.23	0.94	(+) 27650/4.32	0.52
9	(−) 30625/5.97	−0.21	(−) 30630/6.26	−0.20

[a] Expressed as $X \times 10^{-3}$. [b] This transition was not observed in T1D because the spectrum was not taken in this energy region. ND = Not determined.

still react with O_2. From the absorption spectrum in Figure 5B, it is evident that the reduced trinuclear cluster of T1DT3′ Fet3p reacts with O_2 to produce a transient species that is quite similar to that of T1D Fet3p and T1Hg laccase. The similarity of the absorption spectrum of the intermediates in all three enzymes (T1Hg laccase, T1D Fet3p, and T1DT3′ Fet3p) suggests a comparable intermediate species is formed. As with T1Hg laccase and T1D Fet3p, the rate of formation of this transient species was fast and complete at the time the first spectrum was taken (1 min).

The CD spectra of the peroxide intermediate in T1D and T1DT3′ Fet3p were also measured. The ligand field transitions of the T3 Cu are better resolved in CD than in absorption, allowing perturbations of the T3 Cu sites to be followed more closely. Figure 6B shows the CD spectrum of the peroxide intermediate of T1D (**P**-T1D) while Figure 6D shows the CD spectrum of the peroxide intermediate of T1DT3′ (**P**-T1DT3′). In both T1D and T1DT3′ Fet3p, the CD spectrum of the peroxide intermediate is significantly different than that of the resting enzyme (presented in Figure 2). The fact that all of the T3 Cu ligand field transitions are altered indicates that both of the T3 Cu ions are perturbed in the peroxide intermediate.

Nine Gaussian bands are required to simultaneously fit the CD and difference absorption spectrum of T1D-**P** and T1DT3′-**P**. The individual Gaussian bands are presented in Table 4 and are included in Figure 6. Band 7 is required because the absorption spectrum cannot be fit without the presence of this band. Additionally, there is an inflection point in the first derivative of the absorption spectrum, which justifies the presence of a band at ~24 750 cm^{-1} (Figure S1 of the Supporting Information). Band 3 is required because (1) there is a positive band at this energy in the CD spectrum of **P**-T1D; and (2) in **P**-T1DT3′, the absorption spectrum requires the inclusion of a band at this position. Finally, bands 4 and 5 are required to adequately fit the absorption and the negative feature in the CD spectrum (~17 000 cm^{-1}). This derives from the fact that the absorption maximum at 14 500 cm^{-1} is at the inflection point in the CD spectrum.

Based on the energies and high Kuhn anisotropy factors ($\Delta\epsilon/\epsilon$ in Table 4), bands 2−5 are reasonably assigned as T3 Cu ligand field bands. Overall, the ligand fields of T1D-**P** and T1DT3′-**P** are lower than in the corresponding resting enzymes. In the CD spectrum of the resting T3 Cu site, the highest energy ligand field transition was assigned as $d_{x^2-y^2} \rightarrow d_{z^2}$. Previous studies have shown that the T3 Cu sites have an open coordination position in which the peroxide is proposed to bind (*25*). This coordination position is in the *x*,*y*-plane and along the *y* axis. Coordination at this site would increase the energy of the $d_{x^2-y^2}$, d_{z^2}, and d_{yz} orbitals. Because $d_{x^2-y^2}$ would have the greatest overlap with the new ligand, its energy would be expected to increase the most, thereby causing an overall decrease in the ligand field.

The ligand field transitions in T1D-**P** and T1DT3′-**P** are quite similar, indicating a comparable geometric perturbation of the T3 coppers in both intermediates. The largest difference is that in T1DT3′ band 2 shifts to higher energy by ~1070 cm^{-1}. This band is likely related to band 3 of the resting CD spectrum that was assigned as a T3 Cu_α $d_{xy} \rightarrow d_{z^2}$ transition.

The high energies and low Kuhn anisotropy factors of bands 6−9 suggest that these are charge-transfer transitions. Overall, there are no significant differences in the charge-

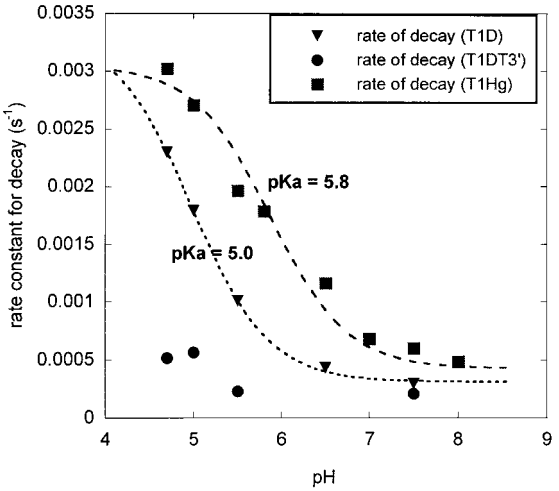

FIGURE 7: pH dependence of the decay of the peroxide intermediate in T1Hg laccase (squares), T1D Fet3p (upside down triangles), and T1DT3′ Fet3p (circles). The data for T1Hg laccase were taken from ref (*15*). The data for T1Hg laccase and T1D Fet3p were fit with the following expression: $k_{obs} = (k_2[H^+] + k_1K_a)/(K_a + [H^+])$. This expression was derived from a protonation equilibrium model.

transfer region of T1D-**P** and T1DT3′-**P**, confirming that the peroxide binds in a similar mode in both systems. In the CD spectrum of resting T1D and T1DT3′ Fet3p, three charge-transfer transitions were observed (one from His to the T2, and two from the μ-OH bridge to the two T3 coppers). In the peroxide intermediate spectrum of T1D and T1DT3′ Fet3p, a minimum of four charge-transfer bands are observed, consistent with the appearance of new peroxide → T3 Cu^{2+} charge-transfer transitions in **P**. While complementary electronic structure calculations are required to assign these transitions, the energies and intensities can be compared to a series of well-characterized complexes to help gain insight into the mode of peroxide binding (see Discussion).

Finally, it should noted that no EPR signal and no ligand field transitions were observed in the MCD spectrum of T1D-**P** and T1DT3′-**P** (Figure S2, Supporting Information), indicating that the T3 coppers are still strongly antiferromagnetically coupled through a bridging ligand. This is consistent with the SQUID magnetic susceptibility and 5 K EPR data on T1Hg laccase-**P**. These earlier studies showed that the antiferromagnetic coupling (−2 J) between the two T3 coppers is >400 cm^{-1} (*14*).

*Decay of **P** in T1D and T1DT3′ Fet3p.* Studies on the peroxide intermediate in T1Hg laccase have shown the decay of **P** involves a one-electron transfer from the T2 Cu to the peroxide with concomitant cleavage of the O−O bond (*15*). This reductive cleavage of the O−O bond was found to yield a native intermediate-like species that further decayed to the resting, oxidized enzyme (*14*). Decay of the peroxide intermediate can be studied by monitoring the absorption intensity of the peroxide charge-transfer band at 340 nm. Figure 5A, inset, shows a sample absorption trace of T1D-**P** at 340 nm as a function of time. The data are fit with a single exponential, allowing the rate of decay to be extracted. The rate of decay of **P** in T1D Fet3p is comparable to the rate in T1Hg laccase (0.0003 s^{-1} at pH 7.5, 25 °C). Figure 5B, inset, shows a sample T1DT3′-**P** absorption trace as a function of time. As in T1D Fet3p and T1Hg laccase, the decay of **P** is fit with a single exponential. In T1DT3′ Fet3p, the rate of decay of **P** is comparable to T1D Fet3p and T1Hg laccase (0.0002 s^{-1} at pH 7.5, 25 °C).

In T1Hg laccase, a residue close to the trinuclear cluster is proposed to protonate at low pH, thereby increasing the rate of decay by 10-fold (*14, 15*). Similar studies on the native intermediate of *Rhus vernicifera* laccase also implicate the involvement of protons in the decay process (*9*), suggesting that protons play an important role in the catalytic cycle. To assess whether the decay of **P** in T1D and T1DT3′ Fet3p is influenced by protons, **P** was prepared at a series of pH's (pH 4.7−7.5), and the rate of decay was measured. As can be seen in Figure 7, the rate of decay of **P** in T1D Fet3p is dependent on pH, and the sigmoidal behavior is consistent with the protonation equilibrium model invoked for T1Hg laccase (included in Figure 7 as a reference). The primary difference is that in T1D Fet3p the pK_a of the protonatable group is lower than in T1Hg laccase (5.0 vs 5.8). In T1DT3′ Fet3p, the decay of **P** did not show the same pH dependence.[8] At high pH, the rate of decay of **P** was about the same as in T1D Fet3p. But at low pH (≤5.5), the rate of decay only increased slightly ($k \sim 0.0005$ s^{-1}) and did not show the same protonation equilibrium behavior.

DISCUSSION

The Electronic Structure of the Trinuclear Cluster and the Role of Hydrogen Bonding. The purpose of this study was to perturb the trinuclear Cu cluster in Fet3p by mutating one of the Cu ligands and to examine how this would influence the O_2 reactivity of the cluster. Interestingly, the $H_{126}Q$ mutation at the T3 Cu site led to changes in the electronic structure of *both* the T3 and the T2 Cu sites. In particular, the mutation results in the following perturbations: (1) One of the T3 Cu_α ligand field[7] bands (d_{xy}) increases in transition energy by ∼500 cm^{-1} in T1DT3′. This increase in transition energy is consistent with a stabilization of the d_{xy} orbital in T1DT3′ because the carbonyl oxygen of Q_{126} is a poorer donor ligand than the imidazole nitrogen. (2) The μ-OH → T3 Cu charge transfer and the antiferromagnetic coupling of the T3 Cu ions are unaltered. (3) Surprisingly, the $H_{126}Q$ mutation also perturbs the T2 Cu site, resulting in a less covalent site. (4) There is also a decrease in charge donation from one of the His ligands to the T2 Cu, suggesting a weaker bonding interaction; this would lead to a decrease in covalency of the T2 site in T1DT3′, as observed by EPR.

As can be seen from the crystal structure of AO in Figure 1, there are a significant number of hydrogen bonds between the T2 and T3 Cu ligands and surrounding residues. Comparing the sequence of AO with other multicopper oxidases reveals that these surrounding residues are highly conserved.[5] Table 1 presents only partial sequence alignments, but it is clear that these hydrogen-bonding residues are almost completely conserved, suggesting that the formed hydrogen-bonding network may make an important contribu-

[8] It should be noted that at low pH a small amount of a second species was observed in T1DT3′. However, this second species did not react with O_2. For intermediate experiments at low pH in T1DT3′, the amount of intermediate formed was normalized to the amount of "reactive protein" present (reactive protein = total protein concentration − amount of second species). At all pHs, the decay of P could be fit with a single exponential, indicating only one species was contributing to the rate.

tion to the stability of the trinuclear Cu cluster in the multicopper oxidases. In the present study, mutation of a T3 Cu ligand alters the electronic structure of the T3 *and* the T2 Cu sites. These changes can be understood if the hydrogen bonding between H_{126} and H_{81} of Fet3p (homologous to H_{104} and H_{60} of AO, Figure 1) is perturbed by substitution of His with Gln. Although the hydrogen bonds are between backbone amides, histidine and glutamine are of different size, and the distance and orientation of the hydrogen-bonding partners would be altered by this mutation. It is interesting to note that the $H_{126}Q$ mutation was also made in the holo enzyme and was catalytically active, exhibiting reduced oxidase and ferroxidase activity.[9] Therefore, it appears this mutation produces a perturbed, but active enzyme.

A fascinating property of T1DT3′ Fet3p is that although one of the T3 Cu histidines (H_{126}) is mutated, the trinuclear cluster remains stable and intact. This can be contrasted with the other two trinuclear mutants ($H_{81}Q$ and $H_{128}Q$) which did not produce a stable trinuclear cluster. H_{81} corresponds to H_{60} in AO and is one of the T2 Cu ligands. Because the carbonyl-O of Gln would be a weaker donor ligand than imidazole, and because the T2 Cu has only two protein-derived ligands, it is not surprising that mutations at the T2 Cu result in an unstable site. However, the instability of the trinuclear cluster in Fet3p with the $H_{128}Q$ mutation is intriguing. H_{128} of Fet3p corresponds to H_{106} of AO. This His is a T3 Cu_β ligand and does have two backbone hydrogen bonds, but they are to residues outside of the trinuclear cluster. Either the T3 Cu_β is inherently less stable than the T3Cu_α, or hydrogen bonds to residues outside of the trinuclear cluster may play a different role than the hydrogen bonds within the cluster. It is possible that the hydrogen bonds between H_{126} and H_{81} (H_{104} and H_{60} in Figure 1) and between H_{416} and H_{483} (H_{448} and H_{506} in Figure 1) help hold the Cu ligands in place, stabilizing the trinuclear cluster. An interesting test of this possibility would be to create the $H_{483}Q$ and $H_{485}Q$ mutants in Fet3p ($H_{506}Q$ and $H_{508}Q$ in AO) to see if the former leads to a stable but perturbed trinuclear cluster while the later leads to cluster instability.

The Nature of the Peroxide Intermediate in Multicopper Oxidases. The trinuclear cluster in T1D Fet3p was found to react with O_2 to form a peroxide intermediate almost identical to the species formed in T1Hg laccase. The perturbed trinuclear cluster in T1DT3′ Fet3p also forms a similar peroxide intermediate. While there are no significant differences in the nature of the intermediate species formed in T1Hg laccase, T1D Fet3p, and T1DT3′ Fet3p, the new CD data in the high-energy region of Fet3p allow further evaluation of possible structural models for the peroxide intermediate.

Previous studies on the peroxide intermediate in T1Hg laccase identified two CT transitions (at 20 700 and 29 400 cm^{-1}) from the absorption spectrum. These were assigned as peroxide $\pi^*_v \rightarrow$ T3 Cu^{2+} and $\pi^*_\sigma \rightarrow$ T3 Cu^{2+} CT, and two possible structural models of the peroxide intermediate were developed (*14*, *25*). The new CD data for Fet3p reveal that there are actually four CT transitions in the peroxide intermediate, allowing these models (shown in Scheme 1) to be further assessed.

[9] Kosman, unpublished results.

Scheme 1

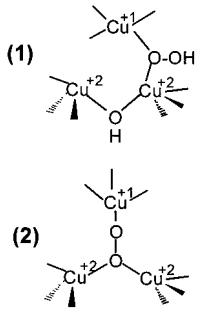

One structural model involves a μ-1,1-hydroperoxide, bridging between the reduced T2 Cu and one of the oxidized T3 Cu ions.[10] This model could give rise to four CT transitions, two peroxide (π^*_v and π^*_σ) $\rightarrow$ T3 Cu and two μ-OH bridge $\rightarrow$ T3 Cu transitions. It should be noted that one of the CT transitions observed in the resting enzyme was attributed to a His $\pi \rightarrow$ T2 Cu CT and would not be observed in the intermediate as the T2 Cu is reduced.

In resting T1D and T1DT3′ Fet3p, the two μ-OH CT transitions are at ~28 000 ($\epsilon \sim 1900\ M^{-1}\ cm^{-1}$) and 30 400 cm^{-1} ($\epsilon \sim 2500\ M^{-1}\ cm^{-1}$), while in the peroxide intermediate of both enzymes, the four CT transitions are at ~20 700 ($\epsilon \sim 1900\ M^{-1}\ cm^{-1}$), 25 000 ($\epsilon \sim 2800\ M^{-1}\ cm^{-1}$), ~27 750 ($\epsilon \sim 5100\ M^{-1}\ cm^{-1}$), and ~30 500 cm^{-1} ($\epsilon \sim 6200\ M^{-1}\ cm^{-1}$). Binding the hydroperoxide to one of the two T3 coppers would cause the two coppers to become more inequivalent. The μ-OH CT to the resultant 5-coordinate Cu would shift ~5000 cm^{-1} to higher energy than the μ-OH CT to the 4-coordinate Cu (*33*). Additionally, the intensity of this higher energy μ-OH CT transition would likely decrease relative to the resting enzyme because the additional hydroperoxide donor would decrease the donor strength of the hydroxide. However, the four CT transitions in the peroxide intermediate are *lower* in energy and *higher* in intensity than the CT transitions in the resting enzymes.

Spectroscopic characterization of mono- and binuclear Cu^{2+}−hydroperoxide complexes reveals that two transitions (π^*_v and π^*_σ) are observed in the energy range of the peroxide intermediate CT transitions. However, in the peroxide intermediate, the ground state of the T3 Cu site is d_{z^2} based on the strong spectral similarity of the T3 ligand field transitions in the intermediate to those of the resting enzyme. Thus, the site maintains a trigonal bipyramidal geometry.[11] Therefore, in the intermediate, the peroxide would interact with the donut of the d_{z^2} orbital, and the intensity of the peroxide $\rightarrow$ Cu CT transitions would be ~3 times lower than in the model complexes, which have a $d_{x^2-y^2}$ ground state (*27*). However, the intensities of the CT transitions in the peroxide intermediate are comparable to or higher than those observed for μ-1,1-hydroperoxide model complexes (*33*, *34*). Therefore, the energies and the intensities

[10] The T2 Cu was shown to be reduced from both the EPR and MCD data. The T3 Cu was shown to be oxidized but antiferromanetically coupled from the CD, SQUID magnetic susceptibility, and He EPR. See ref *14* for details.

[11] The designation of a trigonal pyramidal geometry and d_{z^2} ground state for the T3 site in the peroxide intermediate comes from the facts that: (1) the CD spectrum still shows the same ligand field transitions as the resting T3 site, and (2) there must still be good orbital overlap with the hydroxide bridge to maintain strong antiferromagnetic coupling.

of the CT transitions in the peroxide intermediate do not seem to be consistent with the behavior expected for the CT transitions of the μ-1,1-hydroperoxide-bridged model in Scheme 1.

The second structural model in Scheme 1 involves peroxide binding in a $\mu_3(\eta^1)_3$ mode bridging all three Cu ions in the trinuclear cluster (*25*). This model could also give rise to four CT transitions, two $\times$ 2 peroxide (π^*_v and π^*_σ) $\rightarrow$ T3 Cu^{2+} transitions in the energy region of the intermediate. Unfortunately, there are presently no well-characterized models with a similar binding mode; therefore, electronic structure calculations are needed to assess the viability of this model.

The Role of Protons in Intermediate Decay. Previous studies in T1Hg laccase have examined the detailed mechanism of decay of the peroxide intermediate. It was found that when the enzyme was deprived of 1 electron equiv (i.e., when the T1 Cu is eliminated), decay of P is a slow, one-electron process (*15*). The rate of decay is primarily dependent on the driving force for the $1e^-$ transfer (i.e., the difference in redox potential between the T2 Cu and the peroxide) and the bond dissociation energy of the peroxide (i.e., the strength of the peroxide bond) (*15*). At low pH, this process is proton-assisted, and the rate increases by 10-fold (Figure 7). The rate of **P** decay in T1D and T1DT3′ Fet3p is similar at high pH, indicating that the limited changes in the nature of the T2/T3 cluster have not significantly changed the redox potential of the T2 Cu or the strength of the peroxide bond. However, at low pH, the decay of T1DT3′-**P** is much slower than T1D-**P**. The increase in the rate of decay at low pH has been ascribed to protonation of a nearby residue, likely a highly conserved aspartate (D_{73} in AO, D_{94} in Fet3p) (*14, 15*). In T1Hg laccase, an inverse isotope effect is observed at low pH, indicating that the proton increases the rate of decay by stabilizing the transition state of the decaying intermediate. If the aspartate is the residue responsible for the pH dependence of decay, an intriguing possibility is that it may interact with the T2-bound water, which could participate in this transition state. As can be seen from Figure 1, the carboxylate oxygen atoms of D_{73} in AO are close to and oriented toward the T2-bound water. The altered pH dependence in T1DT3′ Fet3p could indicate that either the properties of the T2-bound H_2O or the interaction between the aspartate and the H_2O has been impacted by the $H_{126}Q$ mutation. Spectroscopic studies reveal that this mutation perturbs both the electronic structure of the T2 Cu and the H-bonding network of the trinuclear cluster. The fact that the peroxide reduction rate can be slowed by mutation suggests that manipulating conditions may allow the peroxide species to be trapped and observed in the native multicopper oxidases to distinguish this step in the molecular mechanism of O_2 reduction. As mentioned earlier, MCD data (*14*) indicate that the peroxide intermediate may be the precursor to the native intermediate in the catalytic cycle, and therefore perturbations of the kinetic behavior and proton dependence might allow more detailed probing of the mechanism in the native enzyme.

In summary, the first perturbed trinuclear Cu cluster has been generated; the perturbation at the T3 also affects the T2 site and demonstrates the strong contribution of H-bonding within the cluster. The perturbed cluster generates an O_2 intermediate very similar to that of the wild-type trinuclear Cu cluster but with significantly different pH-dependent decay kinetics for the reductive cleavage of the O−O bond.

SUPPORTING INFORMATION AVAILABLE

Derivative spectrum of the absorption of the peroxide intermediate in T1D and T1DT3′, and EPR and MCD spectra of the peroxide intermediate in T1D and T1DT3′ Fet3p. This information is available free of charge via the Internet at http://pubs.acs.org.

REFERENCES

1. Solomon, E. I., Sundaram, U. M., and Machonkin, T. E. (1996) *Chem. Rev. 96*, 2563−2605.
2. Askwith, C., Eide, D., VanHo, A., Bernard, P. S., Li, L., Davis-Kaplan, S., Sipe, D. M., and Kaplan, J. (1994) *Cell 76*, 403−410.
3. Hassett, R. F., Yuan, D. S., and Kosman, D. J. (1998) *J. Biol. Chem. 273*, 23274−23282.
4. Silva, D. M. D., Askwith, C., Eide, D., and Kaplan, J. (1995) *J. Biol. Chem. 270*, 1098−1101.
5. Stearman, R., Yuan, D. S., Yamaguchi-Iwai, Y., Klausner, R. D., and Dancis, A. (1996) *Science 271*, 1552−1557.
6. Messerschmidt, A. (1997) *Multi-Copper Oxidases*, World Scientific Publishing Co., River Edge, NJ.
7. Andréasson, L.-E., and Reinhammar, B. (1976) *Biochim. Biophys. Acta 445*, 579−597.
8. Andréasson, L.-E., Brändén, R., and Reinhammar, B. (1976) *Biochim. Biophys. Acta 438*, 370−379.
9. Huang, H., Zoppellaro, G., and Sakurai, T. (1999) *J. Biol. Chem. 274*, 32718−32724.
10. Lee, S. K., George, S. D., Antholine, W. E., Hedman, B., Hodgson, K. O., and Solomon, E. I. (2001) *J. Am. Chem. Soc.*
11. Morie-Bebel, M. M., Morris, M. C., Menzie, J. L., and McMillin, D. R. (1984) *J. Am. Chem. Soc. 106*, 3677−3678.
12. Morie-Bebel, M. M., Menzie, J. L., and McMillin, D. R. (1984) in *Conference on Copper Coordination Chemistry* (Karlin, K. D., and Zubieta, J., Eds.) pp 89−95, Adenine Press, Guilderland, NY.
13. Severns, J. C., and McMillin, D. R. (1990) *Biochemistry 29*, 8592−8597.
14. Shin, W., Sundaram, U. M., Cole, J. L., Zhang, H. H., Hedman, B., Hodgson, K. O., and Solomon, E. I. (1996) *J. Am. Chem. Soc. 118*, 3202−3215.
15. Palmer, A. E., Lee, S.-K., and Solomon, E. I. (2001) *J. Am. Chem. Soc. 23*, 6591−6599.
16. Torres, J., Svistunenko, D., Karlsson, B., Cooper, C. E., and Wilson, M. T. (2002) *J. Am. Chem. Soc. 124*, 963−967.
17. Zoppellaro, G., Sakurai, T., and Huang, H. (2001) *J. Biochem. 129*, 649−653.
18. Blackburn, N. J., Ralle, M., Hassell, R., and Kosman, D. J. (2000) *Biochemistry 39*, 2316−2324.
19. Machonkin, T. E., Quintanar, L., Palmer, A. E., Hassett, R., Severance, S., Kosman, D. J., and Solomon, E. I. (2001) *J. Am. Chem. Soc. 123*, 5507−5517.
20. Felsenfeld, G. (1960) *Arch. Biochem. Biophys. 87*, 247−251.
21. Carithers, R. P., and Palmer, G. (1981) *J. Biol. Chem. 256*, 7967−7976.
22. (1986) *CRC Handb. Chem. Phys. 67*, B-126.
23. Spira-Solomon, D. J., Allendorf, M. D., and Solomon, E. I. (1986) *J. Am. Chem. Soc. 108*, 5318−5328.
24. Cole, J. L., Clark, P. A., and Solomon, E. I. (1990) *J. Am. Chem. Soc. 112*, 9534−9548.
25. Sundaram, U. M., Zhang, H. H., Hedman, B., Hodgson, K. O., and Solomon, E. I. (1997) *J. Am. Chem. Soc. 119*, 12525−12540.
26. Solomon, E. I., and Hanson, M. A. (1999) in *Inorganic Electronic Structure and Spectroscopy: Volume II: Applications and Case Studies* (Solomon, E. I., and Lever, A. B. P., Eds.) John Wiley & Sons, New York.

27. Lever, A. B. P., and Solomon, E. I. (1999) in *Inorganic Electronic Structure and Spectroscopy* (Lever, A. B. P., and Solomon, E. I., Eds.) pp 1−92, John Wiley and Sons, New York.
28. Quintanar, L., Palmer, A. E., Severance, S., Wang, T.-P., Kosman, D. J., and Solomon, E. I. (2002) (manuscript in preparation).
29. Fawcett, T. G., Bernarducci, E. E., Krogh-Jespersen, K., and Schugar, H. J. (1980) *J. Am. Chem. Soc. 102*, 2598−2604.
30. Bernarducci, E. E., Schwindinger, W. F., Hughey, J. L., IV, Krogh-Jespersen, K., and Schugar, H. J. (1981) *J. Am. Chem. Soc. 103*, 1686−1691.
31. McGarvey, B. R. (1966) in *Transition Metal Chemistry* (Carlin, B. L., Ed.) Vol. 3, pp 89−201, Marcel Dekker, New York.
32. Piepho, S. B., and Schatz, P. N. (1983) *Group Theory in Spectroscopy—With Applications to Magnetic Circular Dichroism*, John Wiley and Sons, New York.
33. Chen, P., Fujisawa, K., and Solomon, E. I. (2000) *J. Am. Chem. Soc. 122*, 10177−10193.
34. Root, D. E., Mahroof-Tahir, M., Karlin, K. D., and Solomon, E. I. (1998) *Inorg. Chem. 37*, 4838−4848.
35. Messerschmidt, A., Ladenstein, R., and Huber, R. (1992) *J. Mol. Biol. 224*, 179−205.
36. Messerschmidt, A., Rossi, A., Ladenstein, R., Huber, R., Bolognesi, M., Guiseppina, G., Marchesini, A., Petruzzelli, R., and Finazzi-Agro, A. (1989) *J. Mol. Biol. 206*, 513−529.
37. Ducros, V., Brzozowski, A. M., Wilson, K. S., Brown, S. H., Østergaard, P., Schneider, P., Yaver, D. S., Pedersen, A. H., and Davies, G. J. (1998) *Nat. Struct. Biol. 5*, 310−316.
38. Mikuni, J., and Morohoshi, N. (1997) *FEMS Microbiol. Lett. 155*, 79−84.
39. Zaitseva, I., Zaitsev, V., Card, G., Moshov, K., Bax, B., Ralph, A., and Lindley, P. (1996) *J. Biol. Inorg. Chem. 1*, 15−23.

BI011979J